Journal of the Arkansas Academy of Science

Volume 75 Article 10

2021

Morphology of Rathke's Glands in the Alligator Snapping Turtle, Macrochelys temminckii (Chelonia: Chelydridae)

Stanley E. Trauth
Arkansas State University, trauthse@outlook.com

Morphology of Rathke's Glands in the Alligator Snapping Turtle, Macrochelys temminckii (Chelonia: Chelydridae)

Cover Page Footnote

Collection of turtles was authorized by a scientific collecting permit from the Arkansas Game and Fish Commission (Permit nos. 120820101 in 2011 and 020520134 in 2014). I thank P. Weldon for his helpful comments and information regarding Rathke's glands.

Morphology of Rathke's Glands in the Alligator Snapping Turtle, *Macrochelys temminckii* (Chelonia: Chelydridae)

S.E. Trauth

Department of Biological Sciences, Arkansas State University (Emeritus), State University, AR 72467-0599

Correspondence: strauth@astate.edu

Running Title: Rathke's Glands in the Alligator Snapping Turtle

Abstract

I examined the morphology of Rathke's glands (RG) in the Alligator Snapping Turtle, *Macrochelys temminckii*, using light microscopy and scanning electron microscopy. This species possesses 4 pairs of RG (i.e., an axillary and 3 inframarginals) that are embedded beneath marginal bones and are named primarily according to the anatomical location of their orifices. These holocrine-type, exocrine, integumentary glands are anatomically and ultrastructurally similar to one another. Each gland contains a single and highly vascularized secretory lobule, which is bounded by a thick tunic of asymmetrically arranged striated muscle bundles. Two types of secretory vacuoles were identified within the holocrine cells of the glandular epithelium. The results of this study generally support my previous findings on RG in *Chelydra serpentina*, the Snapping Turtle (ST); however, some lack of cellular and structural conformity was evident compared to glands in this close relative as well as to RG in other turtle species. For example, epithelial cell layer depth and configuration and glandular lumen composition were inconsistent with prior observations. Moreover, the dearth of secretory cells and their products within the lumen of glands suggests that storage or temporary retention of glandular materials differs markedly from the conditions found in RG of other cryptodiran turtle.

Introduction

There are limited detailed descriptions of scent or musk glands, now formally known as Rathke's glands (RG) in turtles, which occur in living members of 13 of the 14 chelonian families (Vallen 1944; Waagen 1972; Ehrenfeld and Ehrenfeld 1973; Solomon 1984; Plummer and Trauth 2009; Trauth and Plummer 2013). Rathke's glands are large, exocrine, integumentary glands, which can number from one to 5 pairs in turtles. Most RG are located in the ventrolateral aspect of the trunk and release a foul-smelling secretion through external epidermal pores. The glands are named based upon either the general location of their pores (i.e., axillary and inguinal) or a pore's proximity to marginal scutes (e.g., 1st, 2nd, or 3rd inframarginal). One or more lobules are sheathed within a thick striated muscle covering; the secretory epithelium is characterized by ovoid-to-spherical holocrine cells (Ehrenfeld and Ehrenfeld 1973; Solomon 1984; Plummer and Trauth 2009; Trauth 2012; Trauth and Plummer 2013; Trauth 2017). Secretions released by these cells are primarily glycoproteins and, to a lesser extent, lipids, as well as various acids (Seifert *et al.* 1994; Weldon *et al.* 2008). The function of RG secretions as well as their comparative anatomy among most chelonians remains largely unknown despite our increasing knowledge about their morphology and glandular chemistry (Weldon *et al*. 2008). Few detailed histological investigations have focused on RG (Zangerl 1941; Ehrenfeld and Ehrenfeld 1973; Solomon 1984; Plummer and Trauth 2009; Trauth 2012; Trauth and Plummer 2013; Trauth 2017).

My primary objective in the present study was to report on the histology and ultrastructure of RG in the *M. temminckii*. The results of this study provide additional information relevant to enhancing knowledge about comparative anatomies of these glands among turtles.

Materials and Methods

I removed the RG from 4 *M. temminckii* collected from northeastern Arkansas and sacrificed with an intra-pleuroperitoneal injection of sodium pentobarbital in accordance with IACUC protocol guidelines at Arkansas State University. The glands were dissected from beneath the marginals (lateral edges of carapace) using a Dremel Multi-Max™ oscillating tool. The RG were then usually bisected into equal halves before fixation in vials of either 10% neutral buffered formalin, NBF (see below for

procedures for paraffin sectioning—LM-Paraffin), and scanning electron microscopy (SEM) for 48 h or in a 2% glutaraldehyde (GTA) solution buffered with 0.1 M sodium cacodylate at a pH of 7.2 (see below for procedures for plastic sectioning—LM-Plastic) for 2 h. For postfixation of GTA-fixed glands, I used 1% w/v osmium tetroxide, buffered as above, for 2 h.

Turtles were sexed, measured (standard carapace length [SCL in mm]), and macro-photographed. Each turtle was assigned an Arkansas State University Museum of Zoology (ASUMZ) number and documented as follows (ASUMZ no., sex, SCL, date of collection): ASUMZ 31793, female, 282 mm, 30 May 2011; ASUMZ 21291, male, 251 mm, 3 June 2011; ASUMZ 33188, female, 327 mm, 2 May 2014, and ASUMZ 33268, 186 mm, 23 August 2014. Turtles were deposited in the herpetological collection in the Arkansas Center for Biodiversity Collections at Arkansas State University.

The RG were prepared for LM-Paraffin, LM-Plastic, and SEM in the former Electron Microscopy Facility at Arkansas State University. Following NBF fixation, the tissues were placed into vials of 70% ethanol and were readied for LM-Paraffin in accordance with the paraffin embedding techniques outlined in Presnell and Schreibman (1997). In brief, the procedures included dehydrating tissue in increasing ethanol solutions (70 to 100%), clearing in 100% xylene, infiltrating in paraffin overnight in a paraffin oven (56°C), embedding in paraffin using plastic molds (glands positioned to yield sagittal sections), sectioning with a rotary microtome into 10 µm serial strips (affixed onto glass microscope slides coated with Haupt's adhesive prior to floating strips in 2% NBF on a slide warmer), and staining using either hematoxylin/eosin (H&E) to reveal general cytology or Pollak trichrome stain (Pollak) for the enhancement of connective tissue and muscle. Cover slips were then adhered to the microscope slides with Permount© (Fisher Scientific Products).

For LM-Plastic for plastic-embedded glands, I cut gland halves into a minimum of 4 pieces, dehydrated gland portions in a graded series of increasing ethanol solutions (50-100%), placed gland tissues in a 50/50% acetone/plastic mixture for overnight infiltration, and then embedded tissues in Mollenhauer's Epon-Araldite #2 (Dawes 1988). For thick sectioning (approximately 1 µm in thickness) and staining, I used glass knives on an LKB Ultrotome (Type 8800) and used Ladd® multiple stain (LMS), respectively.

For SEM, I dehydrated gland halves in a graded series of increasing ethanol solutions (50-100%), followed by several fluid exchanges in 100% ethanol. An Autosamdri-815 critical point drier (Tousimis Research Corporation, Rockville, MD) was used (31°C, 1072 psi, ventilation rate ~100 psi/min) to remove excess ethanol. Gland samples were then mounted on 25.4 mm aluminum pin stub specimen mounts and coated with gold using a Cressington 108 sputter coater (Cressington Scientific Instruments Ltd, Watford, UK). Tissues were then examined using a Vega TS 5136XM digital scanning electron microscope (Tescan USA Inc., Cranberry Township, PA) at 19.5 kV.

For photomicroscopy, I used a Leica MC 120 HD camera atop a Leica DM 2000 LED compound light microscope. For macrophotography, I used a Canon T4i digital single lens reflex camera fitted with a 50 mm autofocus macro lens. Most descriptions of RG anatomy follow the terminology found in Plummer and Trauth (2009), Trauth (2012), Trauth and Plummer (2013), and Trauth (2017). Microscope slides are currently catalogued and housed in the Trauth Histo-herpetology Laboratory located in Morrilton, Arkansas.

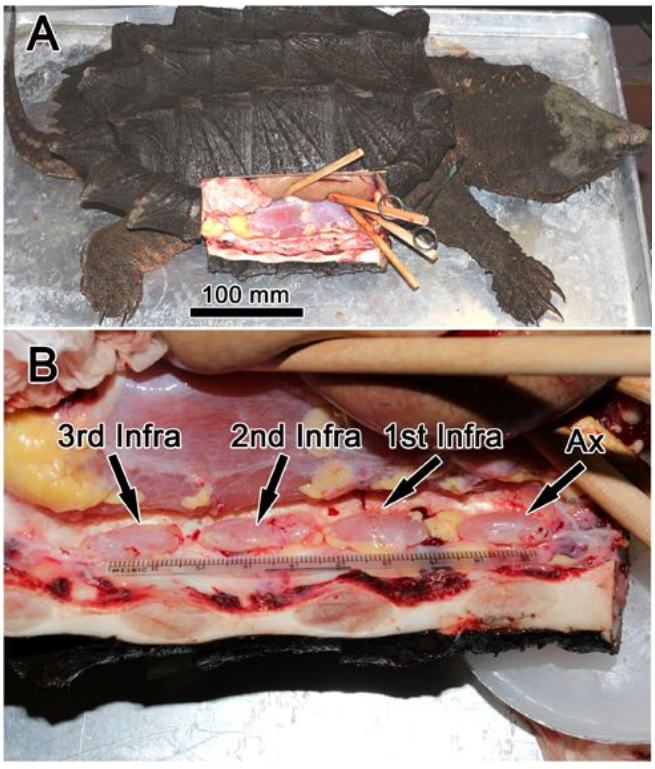

Figure 1. Exposed RG in *M. temminckii* (ASUMZ 33188). A. Dissection of glands using dorsal and lateral incisions into carapace and marginals. B. Arrows identify axillary gland (Ax) and 3 inframarginal glands (1st Infra, 2nd Infra, 3rd Infra) along bridge. Metric ruler is shown below glands in B.

https://scholarworks.uark.edu/jaas/vol75/iss1/10
DOI: 10.54119/jaas.2021.7508

Results

Gross Morphology

The RG of *M. temminckii* are located beneath the posterolateral edge of costal scute 1 (immediately posterior to tip of third rib) and extend to the middle of costal scute 3 between tips of ribs 4 and 6 (Fig. 1). The orifices of these epidermal glands are mostly inconspicuous and were not identified in the present study; however, the three inframarginal orifices are embedded in the posterolateral surfaces of three bridge scutes, whereas the orifice of the axillary gland appears along the interface between abdominal skin and the 4th marginal scute (Waagen 1972). Internally, the glands are aligned in a linear series within slight depressions along the tips of interior marginal bones and are surrounded by a scattering of fatty deposits and loose connective tissue. Gland dimensions are variable, but usually fall between 12 – 20 mm in length, 4 – 6 mm in width, and 3 – 4 mm in depth.

Light Microscopy

The basic internal structure of RG in *M. temminckii* consists of a single lobule, which possesses a secretory epithelium that rests upon a thin basement membrane (Figs. 2; 3A, B). A thick layer of dense connective tissue lies between the lobule and its striated muscle covering (Fig. 2B, C). In general, the secretory epithelium is comprised of a single cell layer, which produces roughly oblong-to-spheroid shaped holocrine cells (Fig. 3). These epithelial cells proliferate outward into the glandular lumen (Fig. 3). At some point following their release from the secretory epithelium, secretory cells lose their structural integrity and degenerate, dumping their cellular contents into the lumen (Fig. 3C). The mostly flocculent cellular debris becomes the material that is eventually passed into a duct leading to the exterior.

Secretory cells are also characterized by the presence of two different types of secretory vacuoles: Type 1 and Type 2 (Fig. 3). Type 1 secretory vacuoles are generally larger than those of Type 2 (Fig. 3B) and appear as singular, mostly spherical masses. Their matrix is not removed during tissue preparation. When stained with LMS, Type 1 secretory vacuoles stain purple in color, a positive indication of the presence of carbohydrate substances.

Type 2 secretory vacuoles, in contrast, are much smaller and appear mostly devoid of material (Fig. 3B,C). Type 2 secretory vacuoles also usually contain

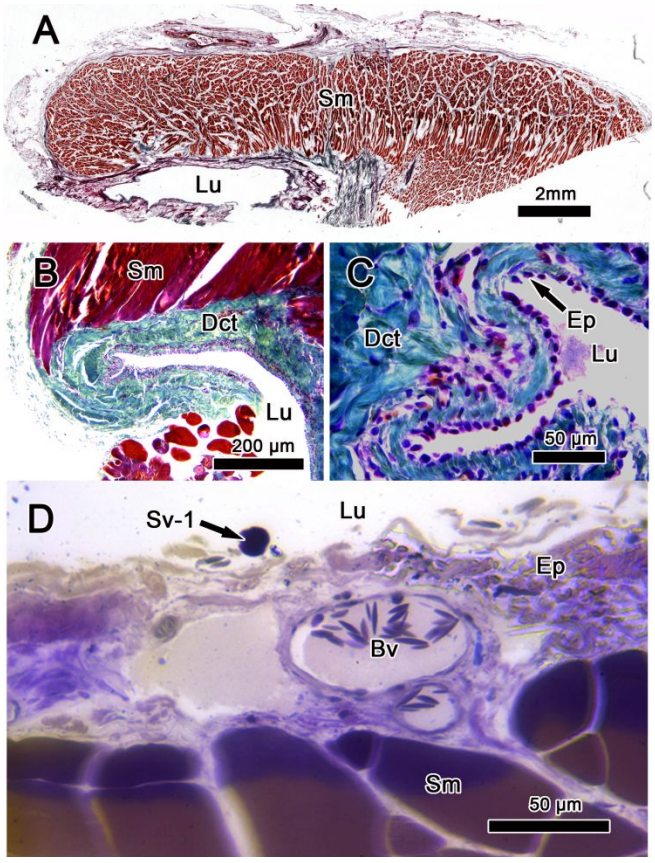

Figure 2. Light micrographs of RG in *M. temminckii*. A. Sagittal section of 2nd inframarginal gland (ASUMZ 21291) showing thick tunic of striated muscle (Sm) and glandular lumen (Lu). Pollak. B. Sagittal section of portion of 3rd inframarginal gland (ASUMZ 33188) showing thick layer of dense connective tissue (Dct) region surrounding lumen. Pollak. C. Magnification of B showing uniformly singular layer of holocrine cells of the secretory epithelium (Ep). Pollak. D. Secretory epithelium of an axillary gland (ASUMZ 31793) subtended by a blood vessel (Bv). A Type 1 secretory vacuole (Sv-1) is identified. LMS.

lipoidal material that is normally referred to as lipid droplets. Soluble lipids within these lipoid droplets are mostly removed from these vacuoles during histological preparation. Although not observed during the present study, osmiophilic, membrane-bound, lipoidal granules are often found within Type 2 secretory vacuoles. Holocrine cell apoptosis releases cellular materials; the persistent presence of the cell's nucleus surrounded by varying levels of glandular constituents characterizes the cellular debris (Fig. 3D).

Scanning Electron Microscopy

When viewed sagittally, secretory lobules of the RG in *M. temminckii* appear to be asymmetrically positioned with respect to their muscular tunic (Fig. 4).

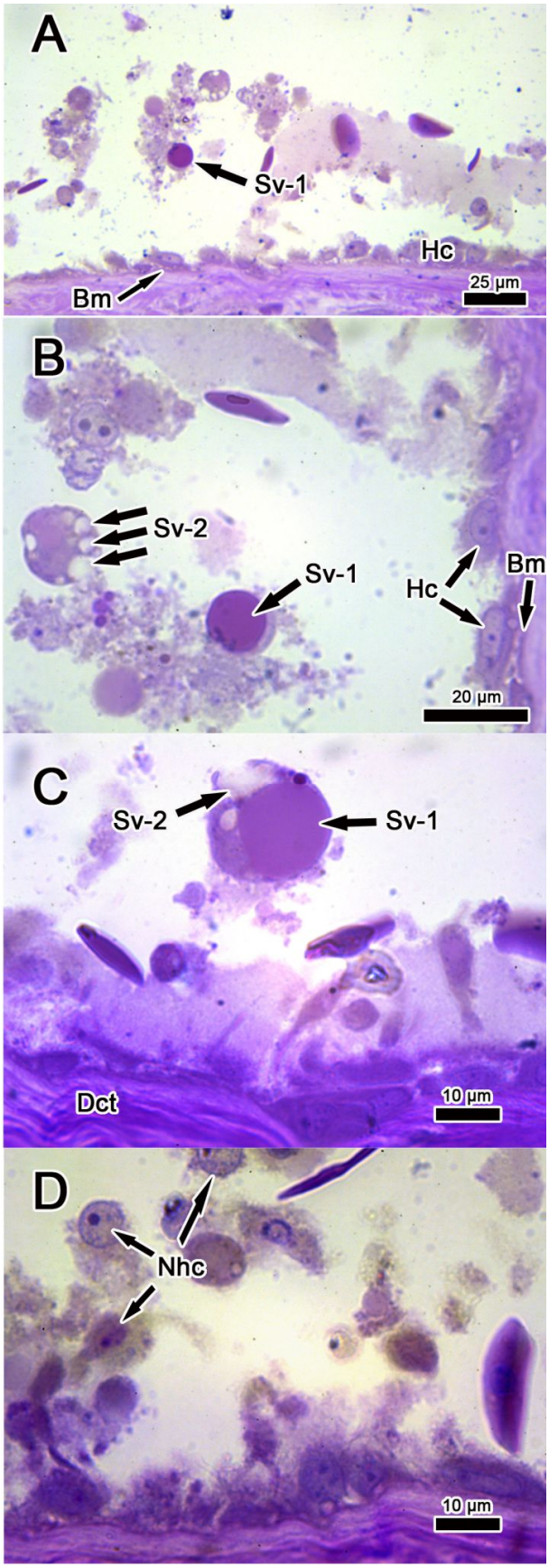

Figure 3. (at left). Light micrographs of the 2nd inframarginal gland in *M. temminckii* (ASUMZ 33268). A. Section showing secretory epithelium with scattered holocrine cells (Hc) along the basement membrane (Bm). A holocrine cell containing a dark-staining, Type 1 secretory vacuole is identified. B. Magnification of A revealing several Type 2 secretory vacuoles (Sv-2) along the periphery of a cell and lying adjacent to a Sv-1. C. Image of a holocrine cell exhibiting Sv-1 and Sv-2. Note that the Sv-2 has ruptured, releasing material into the lumen. D. Image of several holocrine cell nuclei (Nhc) from apoptotic cells. See text for further explanations. LMS for A–D.

The unattached (free) surface of each gland is dominated by a thick mass of striated muscle (exposed surface shown in Fig. 1), whereas the attached surface is comprised primarily of a broad layer of dense connective tissue (Fig. 4B). This dense layer is continuous with the innermost layer of dense connective tissue that encapsulates the lobule (Fig. 2B,C).

A single surface layer of holocrine cells characterized the interior lining of the secretory epithelia in all RG in *M. temminckii* (Fig. 5). Basal cells were not observed using SEM. Numerous intercellar bridges appear to link together all surface cells (Fig. 5A). An abundance of minute, spherical, secretory blebs were observed. Type 1 secretory vacuoles were infrequent (Fig. 5C).

Discussion

Several common morphological and histological features occur in RG found in non-marine turtles studied thus far. For example, the glands of *Sternotherus odoratus* (Ehrenfeld and Ehrenfeld 1973), *Apalone mutica* and *A. spinifera* (Plummer and Trauth 2009), *Kinosternon subrubrum* (Webb 2010), *Chelydra serpentina* (Trauth 2012), *Terrapene carolina* and *T. ornate* (Trauth and Plummer 2013), and *Sternotherus carinatus* (Trauth 2017) exhibit the following shared features: 1) a single lobule or, in exceptional cases, multiple lobules (2 lobules occur in softshell turtles [Plummer and Trauth 2009]) are present; 2) a thin-to-relatively thick layer of dense connective tissue immediately encases the secretory epithelium of a lobule; 3) lobules are wrapped in some manner by a tunic of striated muscle; 4) lobules receive a rich supply of blood from capillaries that lie in close proximity to the basement membrane of the secretory epithelium; 5) holocrine cells of the secretory epithelium generate 2 types of secretory vacuoles, and 6) glandular lobules exhibit lumina packed with either freshly released holocrine cells, previously released apoptotic holocrine cells, and/or cellular debris.

https://scholarworks.uark.edu/jaas/vol75/iss1/10
DOI: 10.54119/jaas.2021.7508

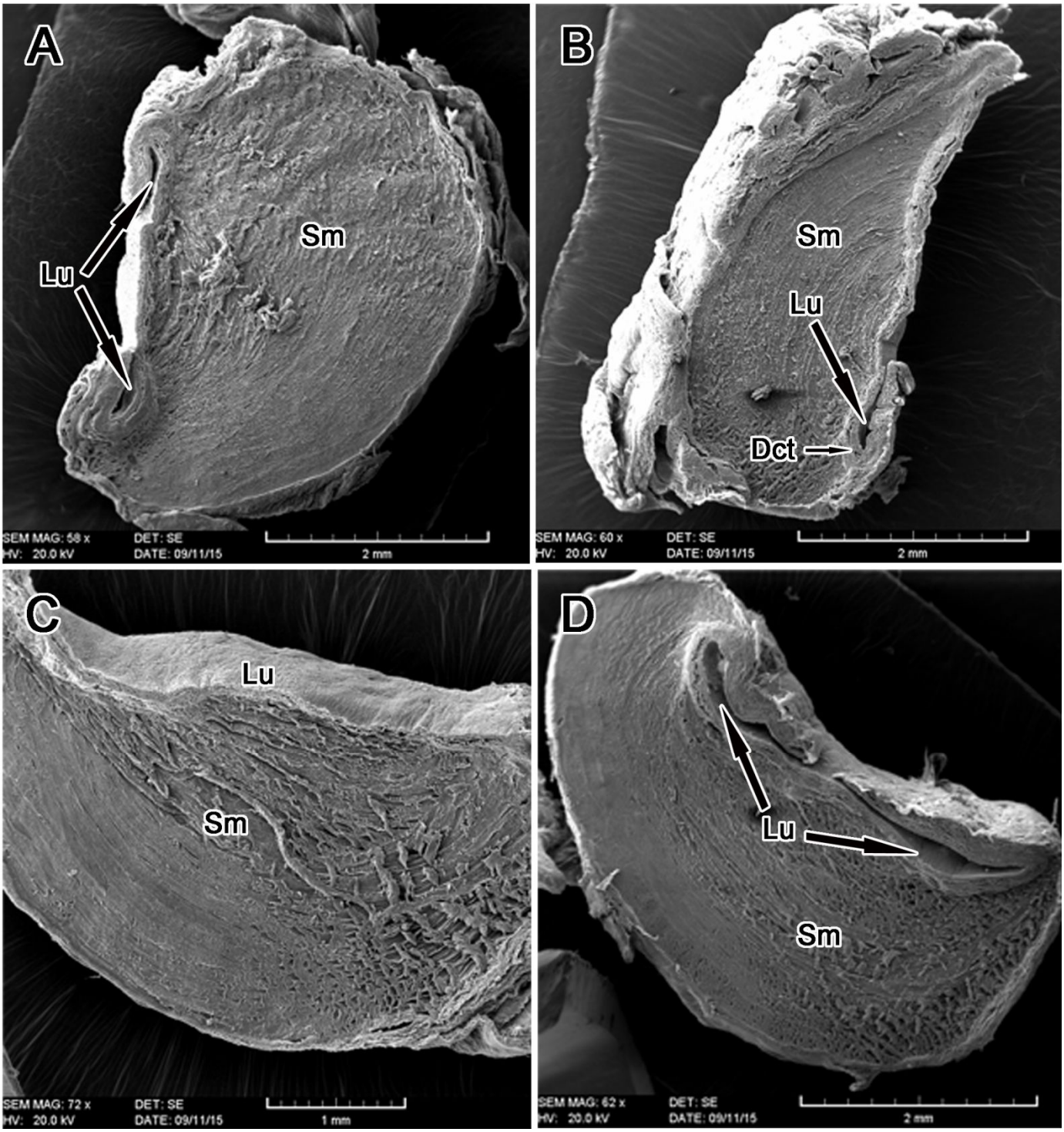

Figure 4. Scanning electron micrographs of sagittal sections (A – D) through the interior of RG in *M. temminckii* (ASUMZ 33188) showing the asymmetrical positioning of the secretory epithelium. A. 1st inframarginal gland. B. 2nd inframarginal gland. C. Axillary gland. D. 3rd inframarginal gland. Abbreviations same as in previous figures.

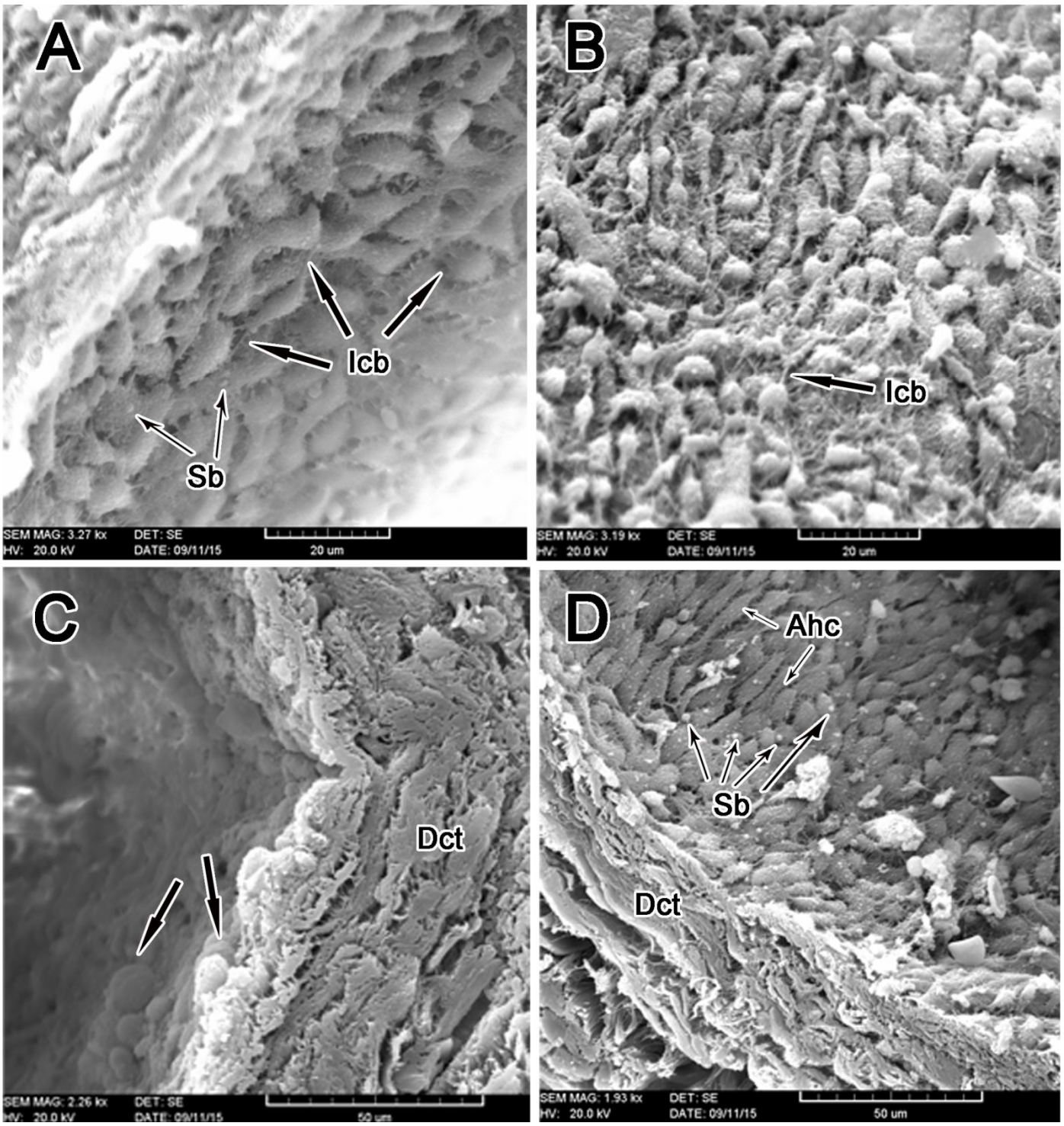

Figure 5. Scanning electron micrographs of the secretory epithelia of RG of *M. temminckii* (same as shown in Figure 4A – D). A. Abundance of intercellular bridges (Icb) radiating between holocrine cells; secretory blebs (Sb) reside on plasma membranes. B. Image reveals intercellular bridges as shown in A. The epithelial lining appears to be a single cell layer. C. Circular secretions, presumably Type 1 secretory vacuoles (arrows), are present. Dct, dense connective tissue. D. Attenuated epithelial cells (Ahc) dominate the surface layer; secretory blebs are numerous.

All *M. temminckii* examined in the present study possess RG that differ in some respect compared to the features listed above, except for some similarities found with *Chelydra serpentina*, the Snapping Turtle

https://scholarworks.uark.edu/jaas/vol75/iss1/10
DOI: 10.54119/jaas.2021.7508

(ST), a closely related species. For example, the lobules of all RG in *M. temminckii* were asymmetrically arranged, being greatly displaced from the core of its muscular tunic. This anatomy was similar to ST; on the other hand, most turtles listed above exhibit centrally located lobules. Another feature, inconsistent with all other turtles (including ST), was the apparent lack of secretory material being stored within lobules in *M temminckii*. This finding was most peculiar and remains equivocal, given that gland preparation for all turtle species employed in 4 previous studies was similar.

The basic morphology of the secretory epithelium was also puzzling when comparing the RG of *M. temminckii* with other turtles. The notable shape and configuration of the single cell layer of holocrine cells, clearly evident in both light and scanning electron micrographs, was remarkably different from the consistency found in turtles species mentioned previously. Also, the microstructure of this single cell layer revealed intercellular bridges, for the first time, by examination using SEM. Transmission electron microscopy will be necessary in order to resolve the nature of the cellular layers, intercellular connections and methods of liberating secretory material from RG in *M. temminckii*.

In conclusion, solving the intricacies related to comparative and functional morphologies of RG will require additional histological and ultrastructural investigations. These methods of inquiry offer a unique opportunity for microscopists to collaborate with behavioral and chemical ecologists.

Acknowledgments

Collection of turtles was authorized by a scientific collecting permit from the Arkansas Game and Fish Commission (Permit nos. 120820101 in 2011 and 020520134 in 2014). I thank P. Weldon for his helpful comments and information regarding Rathke's glands.

Literature Cited

Dawes CJ. 1988. Introduction to biological electron microscopy: theory and techniques. Ladd Research Industries, Inc., Burlington (VT). 315 p.

Ehrenfeld JG and **DW Ehrenfeld.** 1973. Externally secreting glands of freshwater and sea turtles. Copeia 1973:305–14.

Plummer MV and **SE Trauth.** 2009. The structure of Rathke's glands in the softshell turtles *Apalone mutica* and *A. spinifera*. Herpetological Conservation and Biology 4:207-20.

Presnell JK and **MP Schreibman.** 1997. Humason's animal tissue techniques. 5th ed. Johns Hopkins University Press, Baltimore, MD. 572 p.

Seifert WE, SW Gotte, TL Leto, and **PJ Weldon.** 1994. Lipids and proteins in the Rathke's gland secretions of the North American mud turtle (*Kinosternon subrubrum*). Comparative Biochemistry and Physiology 109B:459–63.

Solomon SE. 1984. The characterization and distribution of cells lining the axillary gland of the adult green turtle (*Chelonia mydas* L.). Journal of Anatomy 138:267–79.

Trauth SE. 2012. Morphology of Rathke's glands in the snapping turtle, *Chelydra serpentina*, with comments on the presence of multilaminar lamellar bodies in turtles. Journal of the Arkansas Academy of Science 66:164-72.

Trauth SE. 2017. Histology of Rathke's glands in the razor-backed musk turtle, *Sternotherus carinatus* (Chelonia: Kinosternidae), with comments on lamellar bodies. Journal of the Arkansas Academy of Science 71:35-40.

Trauth SE and **MV Plummer.** 2013. Comparative histology, histochemistry, and ultrastructure of Rathke's glands in hatchlings of two species of North American box turtles (*Terrapene carolina* and *T. ornata*). Chelonian Conservation and Biology 12:268-74.

Vallen E. 1944. Uber die entwicklung der moschusdrűsen bei einigen schildkröten arten. Acta Zoologica 25:1-249.

Waagen GN. 1972. Musk glands in recent turtles. MS Thesis, University of Utah, Salt Lake City, Utah, USA. 64 p.

Webb S. 2010. The histology and histochemistry of Rathke's glands in the Mississippi mud turtle, *Kinosternon subrubrum hippocrepis*. MS Thesis, Arkansas State University, Jonesboro. 37 p.

Weldon PJ, B Flachsbarth, and **S Schulz.** 2008. Natural products from the integument of nonavian reptiles. Natural Products Reports 25:738–56.

Zangerl R. 1941. A series of lateral organs found in embryos of the snapping turtle (*Chelydra serpentina*). Papers of the Michigan Academy of Science Letters 26:339–41.